Possible "umbrella"-like antimagnetic rotation mode in odd-A ^{101,103}Pd and even-even ^{102,104}Pd

H. Jia (贾慧), B. Qi (亓斌),* C. Liu (刘晨), Q. Hu (胡琪), and S. Y. Wang (王守宇)†

Shandong Provincial Key Laboratory of Optical Astronomy and Solar-Terrestrial Environment, School of Space Science and Physics, Institute of Space Sciences, Shandong University, Weihai, 264209, People's Republic of China

(Received 4 July 2017; revised manuscript received 2 December 2017; published 27 February 2018)

The tilted-axis cranking model based on covariant density functional theory is used to study the candidate antimagnetic rotation (AMR) bands in ^{101,102,103,104}Pd. The experimental energy spectra and $B(E2)$ values are reproduced well in the self-consistent and microscopic calculations. By investigating microscopically the composition and orientation of angular momentum, an "umbrella"-like antimagnetic rotation (UAMR) mode resulting from the coupling of four $g_{9/2}$ proton holes to neutron particles is clearly illustrated for the first time.

DOI: 10.1103/PhysRevC.97.024335

I. INTRODUCTION

Antimagnetic rotation (AMR) [1–4] is a rotational phenomenon which has attracted extensive attention. The energy levels in the AMR band differ in spin by $2\hbar$ and are connected by weak electric quadrupole ($E2$) transitions. Another significant feature of the AMR is a decrease of the $B(E2)$ values with increasing spin [5,6]. Since the prediction of AMR in nuclei [1,2], much experimental effort has been devoted to exploring this interesting phenomenon. So far, candidate AMR bands have been reported in the $A \sim 100$ and $A \sim 140$ mass regions [3,7–11]. Lifetime measurements were performed for the AMR bands in ^{105}Cd [12], ^{106}Cd [5], ^{107}Cd [13], ^{108}Cd [14,15], ^{109}Cd [16], ^{110}Cd [17], ^{101}Pd [7–9], ^{104}Pd [10], and ^{142}Eu [11]. ^{109}Cd [18] and ^{110}Cd [17] were suggested to have a strong interplay between the antimagnetic and core rotations.

The AMR bands are usually interpreted in terms of a two-shears mechanism, in which the angular momentum is increased by a simultaneous closing of the two proton-hole blades toward the neutron-particle angular momentum vectors [5,6]. Except for the well-known two-shears mechanism, is it possible that the AMR with more than two shears could exist in a nucleus? In fact, candidate AMR bands have been observed in ^{101}Pd [7–9] and ^{104}Pd [10] ($Z = 46$) with four $g_{9/2}$ proton holes. In addition, we notice that the observed $\Delta I = 2$ bands in the neighboring nuclei ^{102}Pd [19] and ^{103}Pd [20] also exhibit the characteristics of AMR. Therefore, it is interesting to study the possible four-shears mechanism of AMR in the Pd isotopes.

The previously theoretical studies for the candidate AMR bands in Pd isotopes were based on the semiclassical particle rotor model (PRM) and titled-axis cranking (TAC) shell model [7–10,21]. References [7,21] inferred the $\pi g_{9/2}^{-4}$-based configuration for the AMR band of ^{101}Pd within the framework of the PRM. However, Refs. [8,9] favored the $\pi g_{9/2}^{-2}$-based configuration for the AMR band of ^{101}Pd based on the TAC and PRM calculations. In addition, the $\pi g_{9/2}^{-2}$-related configuration for the AMR band of ^{104}Pd [10] was tentatively assigned by analogy with the AMR band of the neighboring nuclei ^{106}Cd [5]. Therefore, it is necessary to investigate the AMR bands in the Pd isotopes by adopting a self-consistent and microscopic model. Recently, covariant density functional theory (CDFT) has succeeded in describing many nuclear properties microscopically [22–34]. Moreover, without any additional parameters, the tilted-axis cranking model based on covariant density functional theory (TAC-CDFT) [3,4,35,36] can self-consistently describe the nuclear rotation excitations. TAC-CDFT has been employed to investigate the magnetic rotation (MR) bands [37–46], the AMR bands [6,18,46–49], and the stapler bands [50,51]. In this work, we adopt the self-consistent and microscopic TAC-CDFT to investigate the candidate AMR bands in Pd isotopes and to explore the possible AMR mechanism generated by closing the four protons blades toward neutrons.

II. THEORETICAL FRAMEWORK

In the TAC-CDFT, the equation of motion for the nucleons derived from the rotating Lagrangian is written as

$$[\boldsymbol{\alpha}\cdot(\boldsymbol{p}-\boldsymbol{V})+\beta(m+S)+V-\boldsymbol{\Omega}\cdot\hat{\boldsymbol{J}}]\psi_k=\epsilon_k\psi_k, \quad (1)$$

where $\hat{\boldsymbol{J}}=\hat{\boldsymbol{L}}+\frac{1}{2}\hat{\boldsymbol{\Sigma}}$ is the total angular momentum of nucleon spinors, and the fields S and V^μ are linked to the densities and current distributions in a self-consistent way. The solution of these equations yields single-particle energies, expectation values of three components $\langle J_i\rangle$ of the angular momentum, energy, quadrupole moments, $B(E2)$ transition probabilities, etc. Moreover, by taking into account the quantal corrections [52], the total angular momentum J calculated corresponds to the quantum number of the angular momentum $I + 1/2$. The detailed formulism can be found in Refs. [3,6,44,45,47]. In the present work, a basis of ten major oscillator shells and the point-coupling interaction parameters PC-PK1 [53] are adopted. Pairing correlations are neglected.

In the microscopic TAC-CDFT calculations, all the energy and angular momentum come from the individual nucleons and there is no core. In the ideal case, the configuration

*bqi@sdu.edu.cn
†sywang@sdu.edu.cn

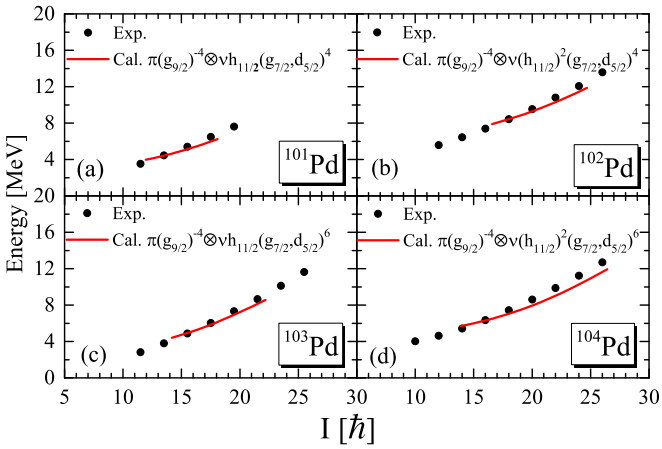

FIG. 1. Excited energies $E(I)$ for the negative-parity sequences in ^{101,103}Pd and positive-parity sequences in ^{102,104}Pd calculated by the TAC-CDFT compared with the experimental data [7,10,19,20]. The energies at $I = 13.5\hbar$, $18\hbar$, $15.5\hbar$, and $16\hbar$ are taken as references for ^{101,102,103,104}Pd, respectively.

should contain the information about all the occupied levels of the nucleons. Usually, the configuration may be simplified by omitting the nucleons in a closure shell, such as in Refs. [6,18,47]. In the present work, the configuration for the AMR band is adopted by setting the ^{100}Sn($Z = 50, N = 50$) as a reference. Therefore, $\pi(g_{9/2})^{-4}$ is taken as the proton configuration, and $\nu(h_{11/2})^m(g_{7/2},d_{5/2})^n$ ($m = 1,2; n = 4,6$) are taken as the neutron configurations for the Pd isotopes ($Z = 46$). The configuration-constrained calculations are performed to keep these configurations.

III. RESULT AND DISCUSSION

The energy spectra, $B(E2)$ values, the ratios of the dynamic moments of inertia $\Im^{(2)}$ to the $B(E2)$ values, deformation parameters, the angular momentum vectors and compositions in ^{101,102,103,104}Pd are calculated and discussed in the following.

The calculated energy spectra $E(I)$ as a function of I in ^{101,102,103,104}Pd are compared with the experimental data in Fig. 1. The data are taken from the "$\nu h_{11/2}$ band" in ^{101}Pd [7], "band 2" in ^{102}Pd [19], "band 1" in ^{103}Pd [20], and the states above $10\hbar$ in ^{104}Pd [10]. It is clear from Fig. 1 that the experimental energy spectra in ^{101,102,103,104}Pd are well reproduced by the present self-consistent calculations at the corresponding spin region. The converged solutions are not

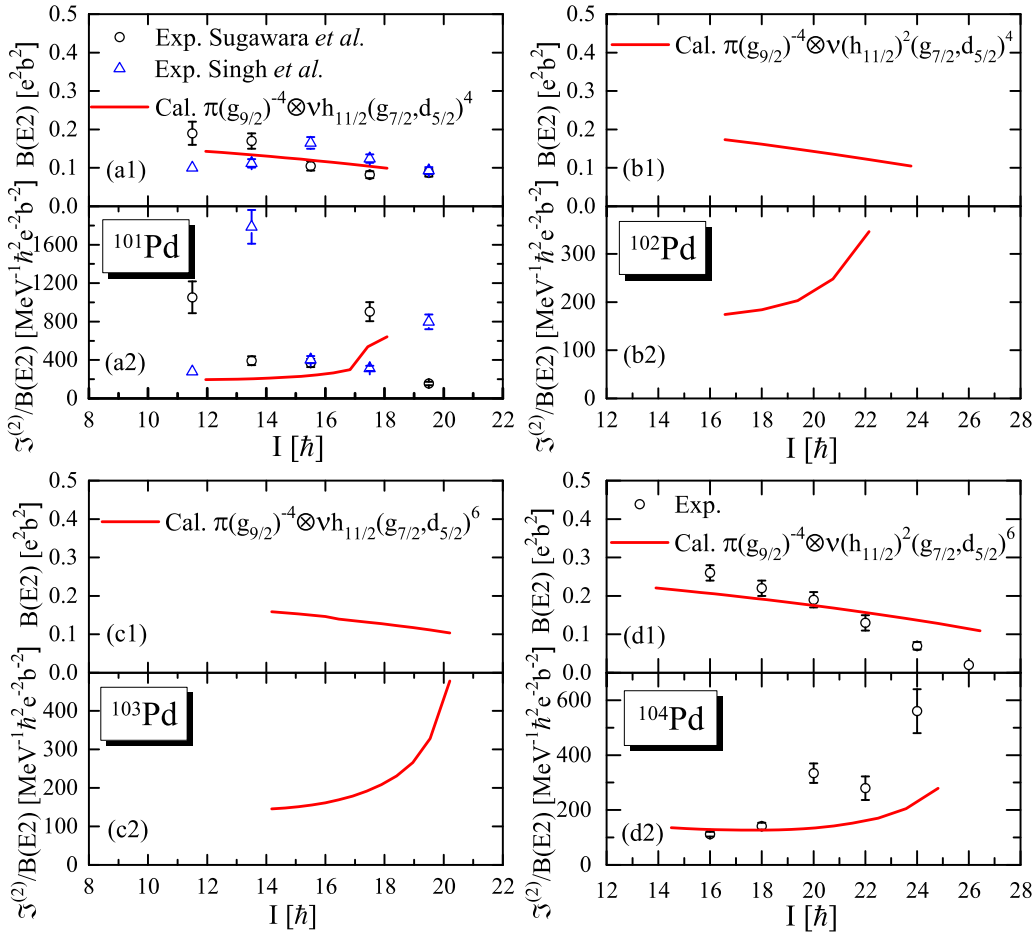

FIG. 2. Calculated $B(E2)$ values and $\Im^{(2)}/B(E2)$ ratios for the $\pi(g_{9/2})^{-4} \otimes \nu h_{11/2}(g_{7/2},d_{5/2})^4$ band in ^{101}Pd, the $\pi(g_{9/2})^{-4} \otimes \nu(h_{11/2})^2(g_{7/2},d_{5/2})^4$ band in ^{102}Pd, the $\pi(g_{9/2})^{-4} \otimes \nu h_{11/2}(g_{7/2},d_{5/2})^6$ band in ^{103}Pd, and the $\pi(g_{9/2})^{-4} \otimes \nu(h_{11/2})^2(g_{7/2},d_{5/2})^6$ band in ^{104}Pd compared with the available experimental data [7–10].

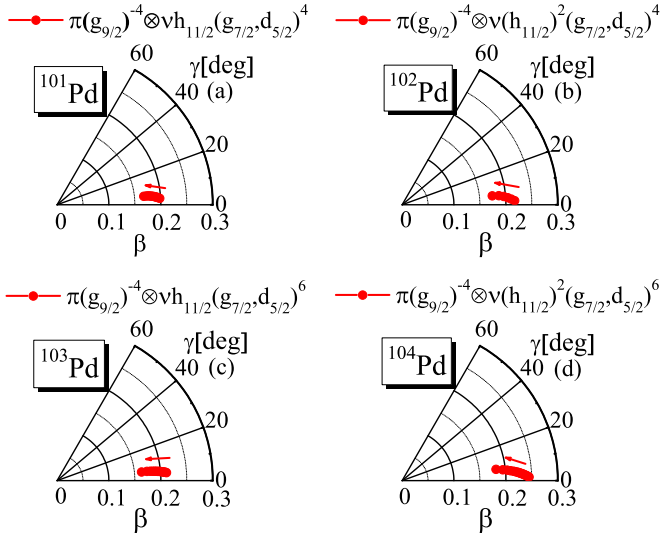

FIG. 3. Evolutions of deformation in the (β,γ) plane with rotational frequency in the TAC-CDFT calculations. The rotational frequencies increase from 0.26 to 0.48 MeV corresponding to the $\pi(g_{9/2})^{-4}\otimes\nu h_{11/2}(g_{7/2},d_{5/2})^4$ configuration in ^{101}Pd, from 0.35 to 0.62 MeV from corresponding to the $\pi(g_{9/2})^{-4}\otimes\nu(h_{11/2})^2(g_{7/2},d_{5/2})^4$ in ^{102}Pd, from 0.36 to 0.64 MeV corresponding to the $\pi(g_{9/2})^{-4}\otimes\nu h_{11/2}(g_{7/2},d_{5/2})^6$ configuration in ^{103}Pd, and from 0.26 to 0.72 MeV corresponding to the $\pi(g_{9/2})^{-4}\otimes\nu(h_{11/2})^2(g_{7/2},d_{5/2})^6$ in ^{104}Pd.

obtained for the lower and higher spin regions in the present TAC-CDFT calculations for the selected configurations.

Typical characteristics of AMR include weak $E2$ transitions, which result in large ratios of the dynamic moments of inertia $\Im^{(2)}$ to the $B(E2)$ values, as well as the decreasing $B(E2)$ values with increasing spin [2,54]. The calculated $B(E2)$ values and $\Im^{(2)}/B(E2)$ as functions of spin are compared with the available experimental data [8–10] in Fig. 2. As shown in Fig. 2, the calculated $B(E2)$ values and $\Im^{(2)}/B(E2)$ ratios are in good agreement with the data in ^{101,104}Pd [8–10]. It should be noted that all the calculated $B(E2)$ values show slight decrease with increasing spin, and the calculated $\Im^{(2)}/B(E2)$ ratios exceed 100 MeV^{-1}(eb)$^{-2}$, which are consistent with the expected characters for AMR [2,54]. Therefore, the present calculations show that the $\pi(g_{9/2})^{-4}\otimes\nu h_{11/2}(g_{7/2},d_{5/2})^4$ band in ^{101}Pd, the $\pi(g_{9/2})^{-4}\otimes\nu(h_{11/2})^2(g_{7/2},d_{5/2})^4$ band in ^{102}Pd, the $\pi(g_{9/2})^{-4}\otimes\nu h_{11/2}(g_{7/2},d_{5/2})^6$ band in ^{103}Pd, and the $\pi(g_{9/2})^{-4}\otimes\nu(h_{11/2})^2(g_{7/2},d_{5/2})^6$ band in ^{104}Pd are AMR bands. It is noted that the bands in ^{102,103}Pd are suggested as the AMR bands for the first time.

We present the evolutions of the calculated deformation for ^{101,102,103,104}Pd in the (β,γ) plane with increasing rotational frequency in Fig. 3. One can see from Fig. 3 that the β values decrease as the rotational frequency increases. The decreasing behavior of the β values is consistent with the decrease of the $B(E2)$ values. Moreover, the calculated β values of ^{101,102,103,104}Pd are all larger than 0.15, which means that the collective rotation should also contribute to the total angular momentum.

To examine the possible AMR mechanism in ^{101,102,103,104}Pd, the angular momentum vectors of the $g_{9/2}$ proton holes (j_π) and the $h_{11/2}$ neutron particles (j_ν) for ^{101,102,103,104}Pd were calculated and presented in Fig. 4. As shown in Fig. 4, the four proton angular momentum vectors of ^{101,102,103,104}Pd divide into two pairs, which are pointing in opposite directions to each other and nearly perpendicular to the angular momentum vectors of neutrons at the initial frequency. With the rotational frequency increasing, the vectors j_π of the four $g_{9/2}$ proton holes gradually align toward the vectors j_ν, and the vectors j_ν of the $h_{11/2}$ neutrons are almost unchanged. The increment of angular momentum is generated by the closing of the two pairs of proton blades toward the neutron angular momentum vectors, and all the four $g_{9/2}$ proton holes contribute to the angular momentum. It presents a picture of the two pairs of shears closing simultaneously. As shown in Fig. 4, the closing of two pairs of shears is similar to the closing of an umbrella. Thus we give the term "umbrella-like antimagnetic rotation" (UAMR) mode to this coupling mechanism. For the higher j orbital (e.g., $i_{13/2}$), the AMR with three pairs of shears is expected, which could be also classified as UAMR mode.

To investigate the umbrella-like antimagnetic rotation (UAMR) mode, the components of the proton and neutron angular momenta in ^{101,102,103,104}Pd are shown in Fig. 5. In the present TAC-CDFT calculations, all of the angular momentum come from the individual nucleons. As shown

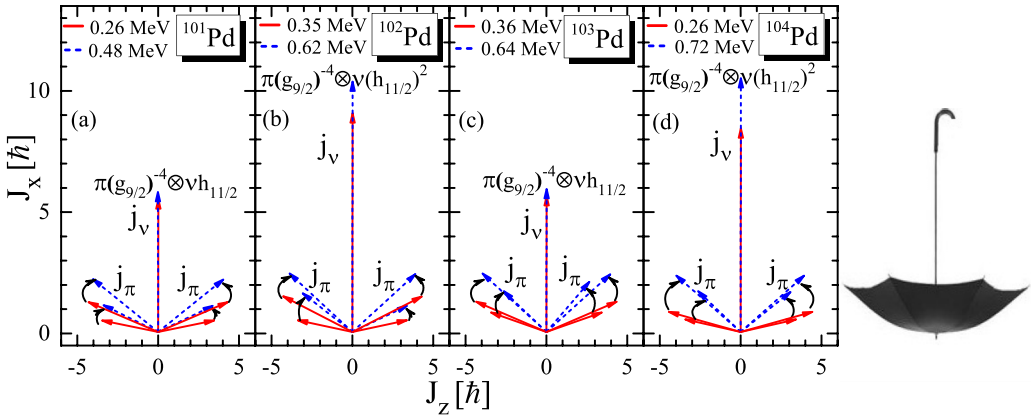

FIG. 4. Angular momentum vectors of the $g_{9/2}$ proton holes (j_π) and the $h_{11/2}$ neutrons (j_ν) in ^{101,102,103,104}Pd.

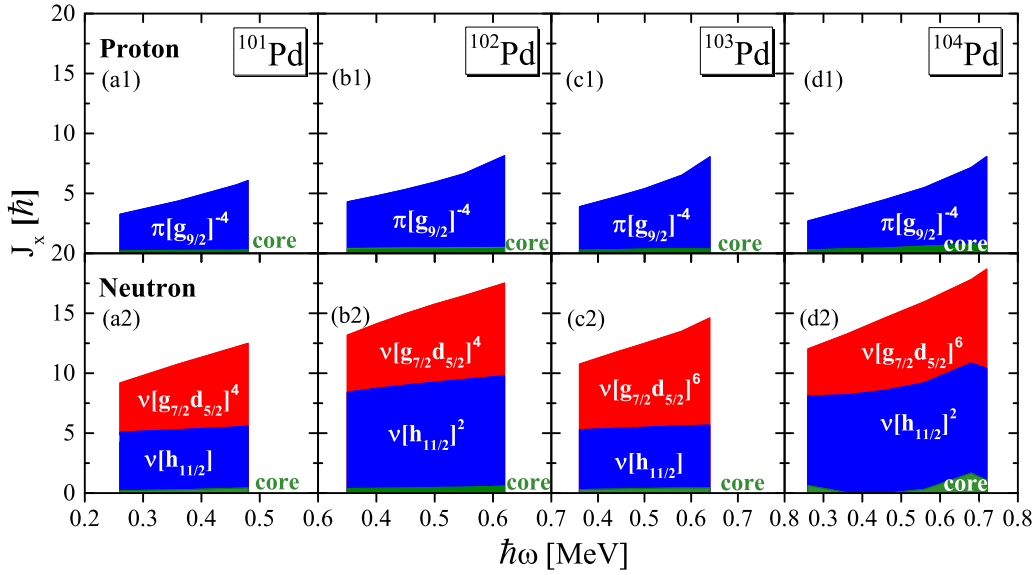

FIG. 5. The compositions of the proton and neutron angular momentum in ^{101,102,103,104}Pd.

in Fig. 5, for the protons, the angular momentum and its increment mainly come from the four proton holes in the $g_{9/2}$ shell, while the $Z = 50$ core barely contributes to the angular momentum. For the neutrons, the angular momentum mainly comes from neutron particles in the $h_{11/2}$ and $(g_{7/2},d_{5/2})$ shells whereas the $N = 50$ core barely contributes to the angular momentum. As the rotational frequency increases, the increment of neutron angular momentum mainly arises from the neutron particles in the $(g_{7/2},d_{5/2})$ shells. We could divide the contribution of the angular momentum into three parts: the AMR mechanism, $\nu(gd)$, and ^{100}Sn core, which are defined by the angular momentum coming from the $g_{9/2}$ proton holes and $h_{11/2}$ neutron particles, the neutrons in the $(g_{7/2},d_{5/2})$ shells, and the orbits below $Z = 50$ and $N = 50$, respectively. The detailed contributions of the AMR, $\nu(gd)$, and ^{100}Sn core for ^{101,102,103,104}Pd are presented in Table I. As shown in Table I, the ^{100}Sn core barely contributes to total angular momentum, which indicates that the ^{100}Sn core stays relatively inert. The

TABLE I. Calculated angular momenta along the x axis (j_x) for the AMR, $\nu(gd)$, ^{100}Sn core, and total angular momenta in ^{101,102,103,104}Pd.

Nuclei	Configuration		$j_x(\hbar)$		Δj_x	Ratio
			$\hbar\omega = 0.26$ MeV	$\hbar\omega = 0.48$ MeV	($\hbar$)	(%)
^{101}Pd	$\pi(g_{9/2})^{-4} \otimes \nu h_{11/2}(g_{7/2},d_{5/2})^4$	AMR	7.94	10.95	3.01	49.1
		$\nu(gd)$	4.11	6.92	2.81	45.8
		^{100}Sn core	0.39	0.71	0.31	5.1
		Total	12.44	18.58	6.13	
			$\hbar\omega = 0.35$ MeV	$\hbar\omega = 0.62$ MeV		
^{102}Pd	$\pi(g_{9/2})^{-4} \otimes \nu(h_{11/2})^2(g_{7/2},d_{5/2})^4$	AMR	11.52	16.38	4.86	59.9
		$\nu(gd)$	4.76	7.71	2.95	36.4
		^{100}Sn core	0.78	1.08	0.30	3.7
		Total	17.06	25.17	8.11	
			$\hbar\omega = 0.36$ MeV	$\hbar\omega = 0.64$ MeV		
^{103}Pd	$\pi(g_{9/2})^{-4} \otimes \nu h_{11/2}(g_{7/2},d_{5/2})^6$	AMR	8.63	12.98	4.35	54.3
		$\nu(gd)$	5.48	8.93	3.45	43.1
		^{100}Sn core	0.56	0.77	0.21	2.6
		Total	14.67	22.68	8.01	
			$\hbar\omega = 0.26$ MeV	$\hbar\omega = 0.72$ MeV		
^{104}Pd	$\pi(g_{9/2})^{-4} \otimes \nu(h_{11/2})^2(g_{7/2},d_{5/2})^6$	AMR	9.89	16.68	6.79	54.2
		$\nu(gd)$	3.91	8.29	4.38	35.0
		^{100}Sn core	0.60	1.96	1.36	10.8
		Total	14.40	26.93	12.53	

contribution from the AMR to total angular momentum is larger than those from the $\nu(gd)$. The contributions from the AMR to total angular momentum increment are 49.1%, 59.9%, 54.3%, and 54.2% for ^{101}Pd, ^{102}Pd, ^{103}Pd, and ^{104}Pd, respectively.

IV. SUMMARY

In summary, we use a fully self-consistent and microscopic TAC-CDFT to investigate the $\pi g_{9/2}^{-4} \otimes \nu h_{11/2}(g_{7/2},d_{5/2})^4$ band in ^{101}Pd, the $\pi g_{9/2}^{-4} \otimes \nu(h_{11/2})^2(g_{7/2},d_{5/2})^4$ band in ^{102}Pd, the $\pi g_{9/2}^{-4} \otimes \nu h_{11/2}(g_{7/2},d_{5/2})^6$ band in ^{103}Pd, and the $\pi g_{9/2}^{-4} \otimes \nu(h_{11/2})^2(g_{7/2},d_{5/2})^6$ band in ^{104}Pd. The calculated energy spectra and $B(E2)$ values are in reasonable agreement with the available data and consistent with the typical characteristics of AMR. By investigating the composition and orientation of the angular momentum, a microscopic picture of the AMR mechanism with two pairs of shears is clearly exhibited for the first time. We give the term umbrella-like antimagnetic rotation (UAMR) mode to the coupling mechanism. It is of great scientific interest to search for the AMR bands with three pairs of shears for the higher j orbits.

ACKNOWLEDGMENTS

The authors express sincere thanks to Dr. P. W. Zhao for the helpful suggestions. This work is partly supported by the National Natural Science Foundation of China (Grants No. 11675094 and No. 11622540), the Shandong Natural Science Foundation (Grant No. ZR2014AQ012), the China Postdoctoral Science Foundation (Grant No. 2017M612254), and Young Scholars Program of Shandong University, Weihai (Grant No. 2015WHWLJH01). The computations were carried out on an HP Proliant DL785G6 server hosted by the Institute of Space Science of Shandong University.

[1] S. Frauendorf, in *Proceedings of the Workshop on Gammasphere Physics, Berkeley, 1995*, edited by M. A. Deleplanque, I. Y. Lee, and A. O. Macchiavelli (World Scientific, Singapore, 1996), p. 272.
[2] S. Frauendorf, Rev. Mod. Phys. **73**, 463 (2001).
[3] J. Meng, J. Peng, S. Q. Zhang, and P. W. Zhao, Front. Phys. **8**, 55 (2013).
[4] J. Meng, S. Q. Zhang, and P. W. Zhao, in *Relativistic Density Functional for Nuclear Structure*, Vol. 10, edited by J. Meng (World Scientific, Singapore, 2016), p. 355.
[5] A. J. Simons, R. Wadsworth, D. G. Jenkins, R. M. Clark, M. Cromaz, M. A. Deleplanque, R. M. Diamond, P. Fallon, G. J. Lane, I. Y. Lee *et al.*, Phys. Rev. Lett. **91**, 162501 (2003).
[6] P. W. Zhao, J. Peng, H. Z. Liang, P. Ring, and J. Meng, Phys. Rev. Lett. **107**, 122501 (2011).
[7] M. Sugawara, T. Hayakawa, M. Oshima, Y. Toh, A. Osa, M. Matsuda, T. Shizuma, Y. Hatsukawa, H. Kusakari, T. Morikawa *et al.*, Phys. Rev. C **92**, 024309 (2015).
[8] V. Singh, S. Sihotra, S. Roy, M. Kaur, S. Saha, J. Sethi, R. Palit, N. Singh, S. S. Malik, H. C. Jain *et al.*, J. Phys. G **44**, 075105 (2017).
[9] V. Singh, S. Sihotra, G. H. Bhat, J. A. Sheikh, M. Kaur, S. Kumar, K. Singh, J. Goswamy, S. Saha, J. Sethi *et al.*, Phys. Rev. C **95**, 064312 (2017).
[10] N. Rather, S. Roy, P. Datta, S. Chattopadhyay, A. Goswami, S. Nag, R. Palit, S. Pal, S. Saha, J. Sethi *et al.*, Phys. Rev. C **89**, 061303(R) (2014).
[11] S. Ali, S. Rajbanshi, B. Das, S. Chattopadhyay, M. S. Sarkar, A. Goswami, R. Raut, A. Bisoi, S. Nag, S. Saha *et al.*, Phys. Rev. C **96**, 021304(R) (2017).
[12] D. Choudhury, A. K. Jain, M. Patial, N. Gupta, P. Arumugam, A. Dhal, R. K. Sinha, L. Chaturvedi, P. K. Joshi, T. Trivedi *et al.*, Phys. Rev. C **82**, 061308(R) (2010).
[13] D. Choudhury, A. K. Jain, G. A. Kumar, S. Kumar, S. Singh, P. Singh, M. Sainath, T. Trivedi, J. Sethi, S. Saha *et al.*, Phys. Rev. C **87**, 034304 (2013).
[14] A. J. Simons, R. Wadsworth, D. G. Jenkins, R. M. Clark, M. Cromaz, M. A. Deleplanque, R. M. Diamond, P. Fallon, G. J. Lane, I. Y. Lee *et al.*, Phys. Rev. C **72**, 024318 (2005).
[15] P. Datta, S. Chattopadhyay, S. Bhattacharya, T. K. Ghosh, A. Goswami, S. Pal, M. Saha Sarkar, H. C. Jain, P. K. Joshi, R. K. Bhowmik *et al.*, Phys. Rev. C **71**, 041305 (2005).
[16] C. J. Chiara, S. J. Asztalos, B. Busse, R. M. Clark, M. Cromaz, M. A. Deleplanque, R. M. Diamond, P. Fallon, D. B. Fossan, D. G. Jenkins *et al.*, Phys. Rev. C **61**, 034318 (2000).
[17] S. Roy, S. Chattopadhyay, P. Datta, S. Pal, S. Bhattacharya, R. K. Bhowmik, A. Goswami, H. C. Jain, R. Kumar, S. Muralithar *et al.*, Phys. Lett. B **694**, 322 (2011).
[18] P. Zhang, B. Qi, and S. Y. Wang, Phys. Rev. C **89**, 047302 (2014).
[19] J. Gizon, B. M. Nyakó, J. Timár, A. Gizon, L. Zolnai, A. J. Boston, Gh. Căta-Danil, J. Genevey, D. T. Joss, N. J. O'Brien *et al.*, Phys. Lett. B **410**, 95 (1997).
[20] B. M. Nyakó, J. Gizon, A. Gizon, J. Timár, L. Zolnai, A. J. Boston, D. T. Joss, E. S. Paul, A. T. Semple, N. J. O'Brien *et al.*, Phys. Rev. C **60**, 024307 (1999).
[21] M. Sugawara, T. Hayakawa, M. Oshima, Y. Toh, A. Osa, M. Matsuda, T. Shizuma, Y. Hatsukawa, H. Kusakari, T. Morikawa *et al.*, Phys. Rev. C **86**, 034326 (2012).
[22] B. D. Serot and J. D. Walecka, Adv. Nucl. Phys. **16**, 1 (1986).
[23] B. A. Nikolaus, T. Hoch, and D. G. Madland, Phys. Rev. C **46**, 1757 (1992).
[24] W. H. Long, N. Van Giai, and J. Meng, Phys. Lett. B **640**, 150 (2006).
[25] P. G. Reinhard, Rep. Prog. Phys. **52**, 439 (1989).
[26] P. Ring, Prog. Part. Nucl. Phys. **37**, 193 (1996).
[27] D. Vretenar, A. V. Afanasjev, G. A. Lalazissis, and P. Ring, Phys. Rep. **409**, 101 (2005).
[28] J. Meng, H. Toki, S. G. Zhou, S. Q. Zhang, W. H. Long, and L. S. Geng, Prog. Part. Nucl. Phys. **57**, 470 (2006).
[29] M. Bender, P. H. Heenen, and P. G. Reinhard, Rev. Mod. Phys. **75**, 121 (2003).
[30] N. Paar, D. Vretenar, and G. Colo, Rep. Prog. Phys. **70**, 691 (2007).
[31] T. Nikšić, D. Vretenar, and P. Ring, Prog. Part. Nucl. Phys. **66**, 519 (2011).
[32] H. Z. Liang, J. Meng, and S. G. Zhou, Phys. Rep. **570**, 1 (2015).
[33] J. Meng and S. G. Zhou, J. Phys. G: Nucl. Part. Phys. **42**, 093101 (2015).

[34] S. G. Zhou, Phys. Scr. **91**, 063008 (2016).
[35] P. W. Zhao, N. Itagaki, and J. Meng, Phys. Rev. Lett. **115**, 022501 (2015).
[36] J. Meng and P. W. Zhao, Phys. Scr. **91**, 053008 (2016).
[37] D. Steppenbeck, R. V. F. Janssens, S. J. Freeman, M. P. Carpenter, P. Chowdhury, A. N. Deacon, M. Honma, H. Jin, T. Lauritsen, C. J. Lister *et al.*, Phys. Rev. C **85**, 044316 (2012).
[38] P. W. Zhao, S. Q. Zhang, J. Peng, H. Z. Liang, P. Ring, and J. Meng, Phys. Lett. B **699**, 181 (2011).
[39] H. Madokoro, J. Meng, M. Matsuzaki, and S. Yamaji, Phys. Rev. C **62**, 061301(R) (2000).
[40] Y. Zheng, J. Li, J. J. Liu, X. G. Wu, H. B. Sun, C. Y. He, C. B. Li, G. S. Li, S. H. Yao, H. W. Li *et al.*, J. Phys. G **42**, 085108 (2015).
[41] J. Li, C. Y. He, Y. Zheng, C. B. Li, K. Y. Ma, and J. B. Lu, Phys. Rev. C **88**, 014317 (2013).
[42] K. Y. Ma, J. B. Lu, D. Yang, H. D. Wang, Y. Z. Liu, J. Li, L. H. Zhu, X. G. Wu, Y. Zheng, and C. Y. He, Eur. Phys. J. A **48**, 82 (2012).
[43] C. B. Li, J. Li, X. G. Wu, X. F. Li, Y. Zheng, C. Y. He, G. S. Li, S. H. Yao, B. B. Yu, X. P. Cao *et al.*, Nucl. Phys. A **892**, 34 (2012).
[44] J. Peng, J. Meng, P. Ring, and S. Q. Zhang, Phys. Rev. C **78**, 024313 (2008).
[45] L. F. Yu, P. W. Zhao, S. Q. Zhang, P. Ring, and J. Meng, Phys. Rev. C **85**, 024318 (2012).
[46] J. Peng and P. W. Zhao, Phys. Rev. C **91**, 044329 (2015).
[47] P. W. Zhao, J. Peng, H. Z. Liang, P. Ring, and J. Meng, Phys. Rev. C **85**, 054310 (2012).
[48] W. J. Sun, H. D. Xu, J. Li, Y. H. Liu, K. Y. Ma, D. Yang, J. B. Lu, and Y. J. Ma, Chin. Phy. C **40**, 084101 (2016).
[49] X. W. Li, J. Li, J. B. Lu, K. Y. Ma, Y. H. Wu, L. H. Zhu, C. Y. He, X. Q. Li, Y. Zheng, G. S. Li *et al.*, Phys. Rev. C **86**, 057305 (2012).
[50] Z. Q. Chen, S. Y. Wang, L. Liu, P. Zhang, H. Jia, B. Qi, S. Wang, D. P. Sun, C. Liu, Z. Q. Li *et al.*, Phys. Rev. C **91**, 044303 (2015).
[51] C. G. Li, Q. B. Chen, S. Q. Zhang, C. Xu, H. Hua, X. Q. Li, X. G. Wu, S. P. Hu, J. Meng, F. R. Xu *et al.*, Phys. Lett. B **766**, 107 (2017).
[52] S. Frauendorf and J. Meng, Z. Phys. A **356**, 263 (1996).
[53] P. W. Zhao, Z. P. Li, J. M. Yao, and J. Meng, Phys. Rev. C **82**, 054319 (2010).
[54] R. M. Clark and A. O. Macchiavelli, Annu. Rev. Nucl. Part. Sci. **50**, 1 (2000).